InGaAs–GaAs 980-nm Stripe-Geometry and Circular Ring Ridge Waveguide Lasers Fabricated With Pulsed Anodic Oxidation

C. Y. Liu, Yi Qu, Shu Yuan, S. Z. Wang, and S. F. Yoon

***Abstract*—$In_{0.22}Ga_{0.78}As$–GaAs quantum-well stripe-geometry and circular ring lasers have been fabricated with pulsed anodic oxidation (PAO). The relationship between ridge heights and laser performance was first studied in the fabrication of stripe lasers. The lowest transparency current density (J_{tr}) of 61.20 A/cm^2 was obtained from the stripe laser with a ridge height of 1.23 μm, corresponding to an etching depth where all the p-doped layers above active region were removed. With the PAO process, when the ridge height (1.77 μm) extended below the active region, J_{tr} is 76.03 A/cm^2, only increased by 24.2%. Based on the experimental results, the circular ring laser, which needs deep etching (below active region) and subsequent PAO, has been fabricated. The fabricated circular ring laser worked under continuous-wave operation at room temperature. Longitudinal mode spacing analysis clearly indicates that the ring resonator is a functional part of the whole circular ring laser.**

***Index Terms*—Circular ring resonator, InGaAs–GaAs, laser diode, pulsed anodic oxidation (PAO).**

I. Introduction

InGaAs–GaAs strained quantum-well (QW) lasers emitting in the 980-nm range are currently used to optically pump erbium-doped fiber amplifiers for telecommunication systems [1], [2]. Because of the simplicity in device processing, ridge waveguide (RW) laser structures have been widely adopted [3]–[5]. The ridge height of an RW laser affects its threshold current density ($J_{\rm th}$) a lot; too small or too large a ridge height will both degrade the device performance [3]. Additionally, since their first demonstration [6], semiconductor ring lasers (SRLs) have received much attention due to their potential applications in photonic integrated circuits [6]–[9]. In the fabrication of SRLs, the ridge height has to be extended below the active region and, thus forming sidewalls that provide large index contrast necessary for guiding the optical mode around "tight" bends [7]. However, conventional SiO_2 deposited by plasma-enhanced chemical vapor deposition (PECVD) may have high chance to damage the exposed active region during the deposition [10]. Pulsed anodic oxidation (PAO) has been proposed and investigated to produce high-quality native oxide on compound semiconductors for laser diode fabrication [11]–[14].

Manuscript received February 9, 2004; revised July 26, 2004.

C. Y. Liu, Y. Qu, and S. Yuan are with the School of Materials Engineering, Nanyang Technological University, Singapore 639798, Singapore (e-mail: liucy@ntu.edu.sg; yqu@ntu.edu.sg; assyuan@ntu.edu.sg).

S. Z. Wang and S. F. Yoon are with the School of Electrical and Electronic Engineering, Nanyang Technological University, Singapore 639798, Singapore (e-mail: eszwang@ntu.edu.sg; esfyoon@ntu.edu.sg).

Digital Object Identifier 10.1109/LPT.2004.839389

In this letter, we report the fabrication of $In_{0.22}Ga_{0.78}As$–GaAs single quantum well (SQW) stripe-geometry Fabry–Pérot (F-P) RW and circular ring lasers with PAO. Laser diode performance versus ridge heights was systematically carried out in the fabrication of stripe-geometry RW lasers. Based on the obtained experimental results, circular ring lasers, with an integrated output stripe defined by using laser direct writing lithography (DWL), wet chemical etching (below QW active region) and subsequent PAO, have been fabricated successfully.

II. Experimental Procedure

$In_{0.22}Ga_{0.78}As$–GaAs graded index separated confinement heterostructure SQW laser structure used in this study was grown by low-pressure metal–organic chemical vapor deposition. The structure is shown in the inset of Fig. 2. Two types of lasers were fabricated from this laser structure, i.e., standard stripe-geometry RW lasers and circular ring lasers. In the fabrication of stripe-geometry RW lasers, following the standard photolithography process, wet chemical etching was carried out with $H_3PO_4 : H_2O_2 : 5H_2O$ to form the ridge. Five samples with identical size (7×7 mm^2) from the same 2-in wafer were etched with different time, resulting in the different etch depths of 0.39, 0.80, 1.23, 1.55, and 1.77 μm (below the QW active region), respectively. With photoresist still on top of the ridge, oxide film with a thickness of 200 ± 5 nm was formed by means of PAO as mentioned in [12]–[14]. Details of laser diode fabrication with PAO have been described in [13]. In the fabrication of circular ring lasers, the major steps were the same as those of stripe-geometry RW lasers fabrication process except that the circular ring pattern was generated by using DWL technique, i.e., a maskless photolithography technique. After fabrication, individual lasers were cleaved for testing without facet coating and intentional heat sink. Laser output power versus injection current (P–I) characteristics were measured at room temperature (RT) under continuous-wave (CW) operation.

III. Results and Discussion

Fig. 1 shows typical RT, CW P–I characteristics of three 1100-μm-long F-P RW InGaAs–GaAs lasers with ridge heights (h) of 0.39, 1.23, and 1.77 μm, respectively. Their $J_{\rm th}$ was 136, 94, and 116 A/cm^2, respectively. Their external quantum efficiency (η_d) was 57.5%, 88.5%, and 77.5%, respectively. The laser with "h" of 1.23 μm presented both the lowest "$J_{\rm th}$" and the highest "η_d." It is clearly seen that the ridge height plays an important role in the device performance. The inset of Fig. 1

1041-1135/$20.00 © 2005 IEEE

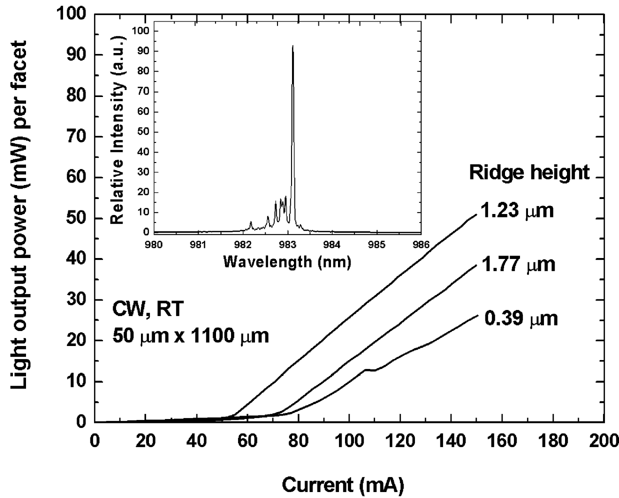

Fig. 1. P–I characteristics of InGaAs–GaAs lasers with different ridge height (h) of 0.39, 1.23, and 1.77 μm, respectively, at RT under CW operation. The cavity length for all the lasers is 1100 μm, with contact ridge width of 50 μm. The inset shows the RT, CW emission spectrum from the fabricated laser.

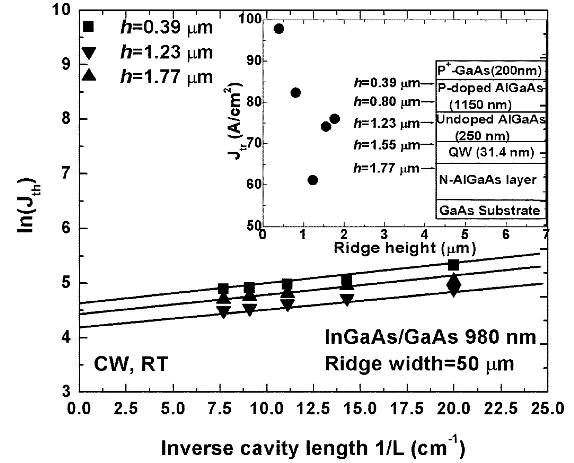

Fig. 2. Logarithm of threshold current density "$\ln(J_{\rm th})$" versus inverse cavity length "$1/L$" for InGaAs–GaAs lasers with different ridge height (h) of 0.39, 1.23, and 1.77 μm, respectively. For each height, the laser cavity length ranged from 500 to 1300 μm. The inset shows transparency current density ($J_{\rm tr}$) of InGaAs–GaAs lasers with different ridge height of 0.39, 0.80, 1.23, 1.55, and 1.77 μm, respectively.

shows the emission spectrum, which is in the 980-nm range, of the fabricated laser diode. From the relationship of reciprocal of "η_d" versus cavity length (L) for F-P RW InGaAs–GaAs lasers, an internal optical loss "α_i" of 3.54 cm^{-1} and average internal quantum efficiency "η_i" of 95.94% were obtained for the InGaAs–GaAs laser structure used in this work.

The "$\ln(J_{\rm th})$" as a function of "$1/L$" is plotted in Fig. 2 for the InGaAs–GaAs F-P RW lasers with different ridge heights. Again, the laser with a ridge height "h" of 1.23 μm showed the lowest threshold current densities for all the cavity lengths. The transparency current density ($J_{\rm tr}$) of the lasers was derived from Fig. 2 using the following equation [15]:

$$\ln J_{\rm th} = \ln\left(\frac{J_0}{\eta_i}\right) + \frac{\alpha_i}{\Gamma g_0} + \frac{L_{\rm opt}}{L} - 1 \qquad (1)$$

where α_i, η_i, Γ, and g_0 are the internal optical loss, internal quantum efficiency, optical confinement factor, and material gain, respectively. The optimum cavity length is defined as $L_{\rm opt} = (1/2\Gamma g_0)\ln(1/R_1R_2)$, and $J_0 = eJ_{\rm tr}$. $R_1 = R_2 = 0.32$ are the optical power reflection coefficients at both facets.

The determined "$J_{\rm tr}$" as a function of "h" is shown in the inset of Fig. 2. The lowest $J_{\rm tr}$ (61.20 A/cm^2) was obtained from the laser with "h" of 1.23 μm, which corresponds to an etching depth where all the p-doped layers on top of the active region were removed. This $J_{\rm tr}$ (61.20 A/cm^2) is close to the theoretically calculated $J_{\rm tr}$ of 43 A/cm^2 for InGaAs–GaAs lasers emitting in the 980-nm range [4]. Lasers with other ridge height such as: $h = 0.39$ μm (etching off the P$^+$-GaAs contact layer), $h = 0.80$ μm (etching stopped in the upper cladding layer), $h = 1.55$ μm (right above the QW), $h = 1.77$ μm (extended below the active region) showed higher $J_{\rm tr}$ than that of the laser with "h" of 1.23 μm. Hu *et al.* [5] has reported that the laser performance is significantly deteriorated when the ridge is extended below the active region due to strong surface recombination. In our case, when the ridge is deeper than the active region, 1.77 μm, $J_{\rm tr}$ is 76.03 A/cm^2, compared with the lowest 61.20 A/cm^2 from "h" = 1.23 μm, increased by only 24.2%. This is presumably attributed to the isolation nature of PAO, since the oxide was formed by consuming a part of semiconductor material, better passivation of the sidewalls after wet etching can be expected. The above results assure of the circular ring lasers fabrication, which needs deep etching and subsequent PAO process.

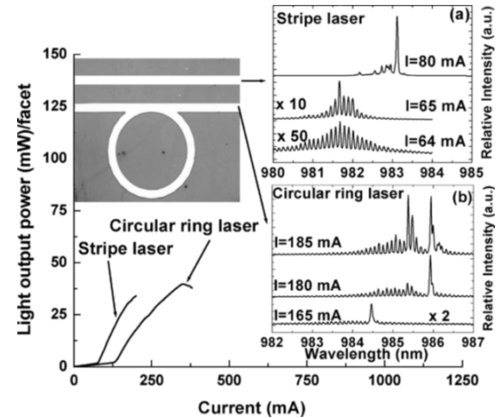

Fig. 3. RT, CW P–I characteristics of InGaAs–GaAs stripe laser and circular ring laser. For both lasers, ridge width is 50 μm and the ridge height is 1.77 μm. Laser cavity length is 1196 μm for the ring laser and 1100 μm for the stripe laser. The inset (left) shows the optical microscopy image of the stripe and circular ring pattern (top view). Radius of the outer ring: $R_{\rm outer} = 250$ μm. Radius of the inner ring $R_{\rm Inner} = 200$ μm. The inset (right) (a) and (b) show the RT, CW emission spectra of the stripe laser and circular ring laser with different injection current, respectively.

Fig. 3 shows RT, CW P–I characteristics of F-P RW laser and circular ring laser from the same wafer. The laser cavity length was 1196 μm for the circular ring laser and 1100 μm for the stripe-geometry laser, with "h" of 1.77 μm for both lasers. The inset (left) of Fig. 3 shows the top view optical microscopy image of the circular ring pattern with an outer radius of 250 μm, an inner radius of 200 μm, respectively, the contact ridge width is 50 μm for both the ring and the stripe. The stripe and ring lasers had $J_{\rm th}$ of 126.7 A/cm^2, 105.87 A/cm^2, respectively. The slope efficiency is 0.285 W/A per facet for the ring laser, and 0.49 W/A per facet for the stripe laser, respectively. Insets (right) Fig. 3(a) and (b) show the emission spectra of the F-P laser and circular ring laser under different injection currents, respectively. With injection current increasing, a primary mode dominated in the stripe-geometry laser, but two competing modes

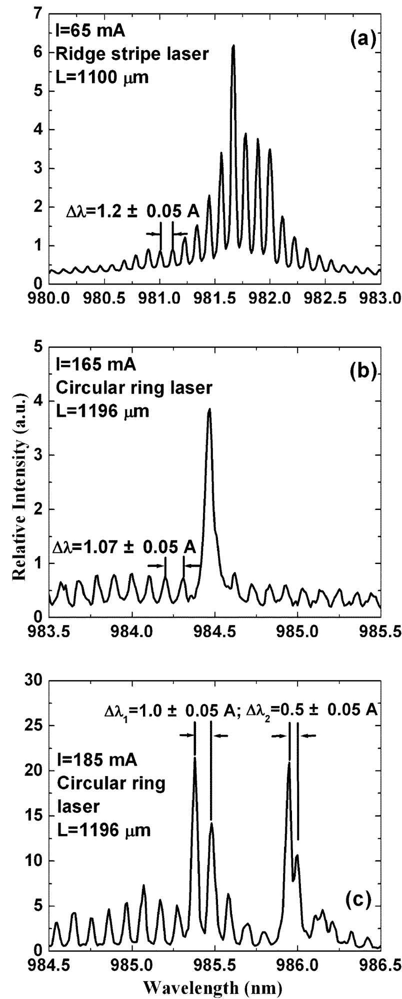

Fig. 4. RT, CW longitudinal mode spectra of stripe laser with injection current of (a) 65 mA and circular ring laser with injection current of (b) 165 and (c) 185 mA, respectively. For both lasers, ridge width is 50 μm and the ridge height is 1.77 μm. Laser cavity length is 1196 μm for the circular ring laser and 1100 μm for the stripe laser.

coexisted in the circular ring laser as shown in insets Fig. 3(a) and (b), respectively. To determine where these modes are from, the longitudinal mode spacing of both stripe-geometry laser and circular ring laser was calculated, as shown in the following.

Fig. 4(a) presents the longitudinal mode spectra of stripe-geometry lasers and that of circular ring lasers with injection current of (b) 165 and (c) 185 mA, respectively. For Fig. 4(a), whose $\Delta\lambda$ was 1.2 $\pm$ 0.05 Å, which agrees extremely well with the calculated value of 1.22 Å, obtained by applying the $\Delta\lambda = \lambda^2/2LN_{\rm eff}$ ($N_{\rm eff} = 3.6$, $L = 1100$ μm). For the circular ring laser, when applying the equation $\Delta\lambda = \lambda^2/2LN_{\rm eff}$, $L = L_s$ or $L = L_s + L_c$, where L_s stands for the cavity length of stripe and L_c stands for the circumference of the circular ring part. From Fig. 4(b), the measured value of $\Delta\lambda$ was 1.07 ± 0.05 Å, which corresponds to the calculated $\Delta\lambda$ of 1.12 Å when we adopt $L = L_s = 1196$ μm. When the injection current is increased to 185 mA, the longitudinal mode spacing is obviously different, as shown in Fig. 4(c). From Fig. 4(c), $\Delta\lambda_1 = 1.0 \pm 0.05$ Å, $\Delta\lambda_2 = 0.5 \pm 0.05$ Å, it means that $\Delta\lambda_1$ still corresponds to the $\Delta\lambda = \lambda^2/2LN_{\rm eff}$ ($L = L_s = 1196$ μm) based on earlier discussion, while $\Delta\lambda_2$ corresponds to the calculated $\Delta\lambda = \lambda^2/2LN_{\rm eff}$ ($L = L_s + L_c$, $L_c = 2 \times \pi \times 225$ μm) which is 0.52 Å. This observation clearly indicates that the ring resonator is a functional part of the whole cavity when the injection current reaches a certain degree.

IV. Conclusion

$In_{0.22}Ga_{0.78}As$–GaAs SQW stripe-geometry RW and circular ring lasers have been fabricated with PAO. The lowest $J_{\rm tr}$ of 61.20 A/cm^2 was obtained from the stripe-geometry laser with ridge height of 1.23 μm, which corresponds to an etching depth where all the p-doped layers above the active region were removed. The fabricated circular ring laser worked under RT, CW operation with a $J_{\rm th}$ of 105.87 A/cm^2, a slope efficiency of 0.285 W/A per facet. Longitudinal mode spacing analysis clearly indicates that the ring resonator is a functional part of the whole circular ring laser.

References

[1] Y. K. Chen, M. C. Wu, W. S. Hobson, S. J. Pearton, A. M. Sergent, and M. A. Chin, “High-power 980-nm AlGaAs/InGaAs strained quantum-well laser grown by OMVPE,” *IEEE Photon. Technol. Lett.*, vol. 3, no. 5, pp. 406–408, May 1991.

[2] J. H. Lee, W. J. Lee, and N. Park, “Comparative study of temperature dependent multichannel gain and noise figure distortion for 1.48- and 0.98-μm pumped EDFAs,” *IEEE Photon. Technol. Lett.*, vol. 10, no. 12, pp. 1721–1723, Dec. 1998.

[3] C. P. Chao, S. Y. Hu, K. Law, B. Young, J. L. Merz, and A. C. Gossard, “Low threshold InGaAs/GaAs strained layer single quantum well laser with simple ridge waveguide structure,” *J. Appl. Phys.*, vol. 69, no. 11, pp. 7892–7894, Jun. 1991.

[4] S. Y. Hu, D. B. Young, S. W. Corzine, A. C. Gossard, and L. A. Coldren, “High efficiency and low-threshold InGaAs/AlGaAs quantum-well lasers,” *J. Appl. Phys.*, vol. 76, no. 6, pp. 3932–3934, Sep. 1994.

[5] S. Y. Hu, D. B. Young, A. C. Gossard, and L. A. Coldren, “The effect of lateral leakage current on the experimental gain/current-density curve in quantum-well ridge-waveguide lasers,” *IEEE J. Quantum Electron.*, vol. 30, no. 10, pp. 2245–2250, Oct. 1994.

[6] A. S. Liao and S. Wang, “Semiconductor injection lasers with a circular resonator,” *Appl. Phys. Lett.*, vol. 36, no. 10, pp. 801–803, May 1980.

[7] M. R. Krames, A. D. Minervini, and N. Holonyak Jr., “Deep-oxide curved resonator for low-threshold AlGaAs-GaAs quantum well heterostructure ring lasers,” *Appl. Phys. Lett.*, vol. 67, no. 1, pp. 73–75, Jul. 1995.

[8] G. Griffel, J. H. Abeles, R. J. Menna, A. M. Braun, J. C. Connolly, and M. King, “Low -threshold InGaAsP ring lasers fabricated using bi-level dry etching,” *IEEE Photon. Technol. Lett.*, vol. 12, no. 2, pp. 146–148, Feb. 2000.

[9] M. Sorel, G. Giuliani, A. Scire, R. Miglierina, S. Donati, and P. J. R. Laybourn, “Operating regimes of GaAs-AlGaAs semiconductor ring lasers: Experiment and model,” *IEEE J. Sel. Topics Quantum Electron.*, vol. 39, no. 10, pp. 1187–1195, Oct. 2003.

[10] A. S. W. Lee, D. A. Thompson, and B. J. Robinson, “Enhanced bandgap blue-shift in InGaAsP multiple-quantum-well laser structures by low-temperature-grown InP,” *Semicond. Sci. Technol.*, vol. 15, pp. L41–L43, Dec. 2000.

[11] M. J. Grove, D. A. Hudson, P. S. Zory, R. J. Dalby, C. M. Harding, and A. Rosenberg, “Pulsed anodic oxides for III-V semiconductor device fabrication,” *J. Appl. Phys.*, vol. 76, no. 1, pp. 587–589, Jul. 1994.

[12] C. Y. Liu, S. Yuan, J. R. Dong, S. J. Chua, M. C. Y. Chan, and S. Z. Wang, “Temperature-dependent photoluminescence of GaInP/AlGaInP multiple quantum well laser structure grown by metalorganic chemical vapor deposition with tertiarybutylarsine and tertiarybutylphosphine,” *J. Appl. Phys.*, vol. 94, no. 5, pp. 2962–2967, Sep. 2003.

[13] C. Y. Liu, S. F. Yoon, S. Z. Wang, W. J. Fan, Y. Qu, and S. Yuan, “Fabrication of high-performance InGaAsN ridge waveguide lasers with pulsed anodic oxidation,” *IEEE Photon. Technol. Lett.*, vol. 16, no. 11, pp. 2409–2411, Nov. 2004.

[14] S. Yuan, C. Jagadish, Y. Kim, Y. Chang, H. H. Tan, R. M. Cohen, M. Petravic, L. V. Dao, M. Gal, M. C. Y. Chan, E. H. Li, S. O. Jeong, and P. S. Zory Jr., “Anodic oxide induced intermixing in GaAs/AlGaAs quantum well and quantum wire structures,” *IEEE J. Sel. Topics Quantum Electron.*, vol. 4, no. 4, pp. 629–635, Jul./Aug. 1998.

[15] S. L. Chuang, *Physics of Optoelectronic Devices*. New York: Wiley, 1995.